



**HAL**  
open science

# A shadow fault detection method based on the standard error analysis of I-V curves

Mickael Bressan, Youssef El Basri, A.G. Galeano, Corinne Alonso

## ► To cite this version:

Mickael Bressan, Youssef El Basri, A.G. Galeano, Corinne Alonso. A shadow fault detection method based on the standard error analysis of I-V curves. *Renewable Energy*, 2016, *Renewable Energy*, 99, pp.1181-1190. 10.1016/j.renene.2016.08.028 . hal-01962964

**HAL Id: hal-01962964**

**<https://laas.hal.science/hal-01962964>**

Submitted on 9 Jan 2019

**HAL** is a multi-disciplinary open access archive for the deposit and dissemination of scientific research documents, whether they are published or not. The documents may come from teaching and research institutions in France or abroad, or from public or private research centers.

L'archive ouverte pluridisciplinaire **HAL**, est destinée au dépôt et à la diffusion de documents scientifiques de niveau recherche, publiés ou non, émanant des établissements d'enseignement et de recherche français ou étrangers, des laboratoires publics ou privés.

# A shadow fault detection method based on the standard error analysis of I-V curves

M. BRESSAN<sup>1</sup>, Y. EL BASRI<sup>1</sup>, A. G. GALEANO<sup>3</sup>, C. ALONSO<sup>1,2</sup>

<sup>1</sup> CNRS; LAAS; 7 Avenue du Colonel Roche, F-31077, TOULOUSE, FRANCE.

<sup>2</sup> UNIVERSITE DE TOULOUSE; UPS, INSA; LAAS; F-31400, TOULOUSE, FRANCE.

<sup>3</sup> Department of Electrical and Electronic Engineering, Universidad de los Andes, Bogotá, Colombia

E-mail: michael.bressan@laas.fr, corinne.alonso@laas.fr

Abstract: Shading on photovoltaic (PV) modules induces disproportionate impacts on power production. This paper presents a fault detection method able to identify anomalies on PV systems such as shading problems. The presence of localized shading on PV modules leads to an overheating of the shaded PV cells despite the activation of by-pass diodes. The temperature increase reduces considerably PV module performances and its lifetime. The presented method uses a simple equation, which corresponds to the normalized error (DE) of the comparison between the I-V curve in normal operation and the I-V curve in shading condition. The first derivative calculation gives the area of the detection in function of the PV voltage of the module (DE/DV). This defines whether one or several PV cells dissipate power. This phenomenon essentially occurs in the case of non-uniform irradiance received on PV modules and could impact PV modules performances. The detection method is explained in detail through the study of specific shadows simulations on PV modules. The results are validated through experimental tests on PV modules.

Keywords: Thermal dissipation, I-V curves analysis, shading problems, first derivative calculation, fault detection

## 1. Introduction

In recent years, photovoltaic (PV) modules have become a popular source of energy in both commercial and residential applications. This energy source has received much attention as an alternative form of electricity generation and is commonly present on buildings throughout the World.

Generally, PV modules are arranged in a way that maximizes the density of modules per unit of area rather than maximizing their efficiency. As a result, the incidence of shading over several modules is common in all applications, causing losses [1-2]. There are several causes of shading such as trees, adjacent buildings or soiling [3-4]. It is important to detect these failures because of partial shading can lead an annual 10-20% reduction in power production or more in residential installations [5], due to both reduced irradiance on PV modules. Soiling may have a large effect on efficiency decreasing PV performances. Some studies [6-8] quantify performance decrease due to soiling. The study of Soteris [9] shows soiling affects seriously the performance of PV panels and it is necessary to clean immediately PV panels after dust episode. When a part of a PV module is shaded, some of its cells may work in reverse bias and reach breakdown voltage. The covered PV cells dissipate thermal power with the temperature increase. In extreme cases, this situation may lead to hot-spot problems, causing irreversible damage to the system. In order to protect shaded solar cells from breakdown voltage, commercial modules are equipped with by-pass diodes [10]. However, these by-pass diodes deform the I-V curves of the shaded modules when diodes are activated.

39 Many authors have proposed solutions and algorithms to detect several failures on PV systems as hot-spot  
40 formation, soiling and aging degradation [11-13]. The electric method such as time domain reflectometry is able  
41 to detect failure position in PV cell string but it is not able to identify clearly if a shadow anomalies is present such  
42 as soiling. The study proposed by Hirata [13] consists in acquire I-V curves of PV modules string under low  
43 irradiance in order to detect parameter variation on series resistance, shunt resistance and diode factor. Based on  
44 this study, it exists a real interest to develop a method of fault detection able to prevent about shading problems  
45 and temperature increases despite the activation of the bypass diodes. It is important to investigate this problem  
46 because PV system are already confronted to shading problems in real operating.

47 It exists method able to detect online failures of PV systems and more particularly defects as shadows [14]. They  
48 all have a common point: the need of a proper shadow detection method. The first work [15] consisted of detecting  
49 the activation of bypass diodes. However, this is not enough to ensure a proper function of the PV cell. The  
50 presented method consists in detecting the activation of by-pass diode due to some shading scenario by calculating  
51 the first derivative ( $DI/DV$ ) and the second derivative ( $DI^2/DV^2$ ). But this method does not permit to clearly  
52 identify if the shading is uniform or not on PV module. Moreover, it does not detect if a thermal dissipation  
53 problem of the covered PV cells exists despite the activation of the bypass diode.

54 In this paper, the presented shadow detection method consists in comparing I-V curves in normal operation issue  
55 to a validated solar model with I-V curves in shaded operation. The error issued from this comparison is normalized  
56 and derived in order to calculate a direct derivative in function of the PV module voltage. The main objective of  
57 this detection is to accurately identify anomalies such as shading problems on PV modules. The presence of  
58 localized shading on PV module causes a significantly temperature increase impacting PV performances and the  
59 PV module lifetime despite the activation of the by-pass diodes. This phenomenon is essentially characterized by  
60 a non-uniform shading. The difference of the I-V curves shape for each case of shading sets will permit to  
61 dissociate more easier an homogeneous shading of a non homogeneous and will facilitate the fault detection and  
62 the identification of the shadow anomaly. Moreover, this detection method should not perturb the PV production  
63 and it may operate with no need to be disconnected from its load thanks to an autonomous online I-V tracer [16].  
64 For this study, and to validate the presented method, the I-V curves are traced using MP-160 I-V tracer (3kW).  
65 This paper is organized as follows, section 2 presents the necessity to develop a model considering the effect of  
66 shading on I-V curves. Moreover, some localized shading sets on PV module are performed to see the abnormal  
67 temperature increase of the shaded PV cell. The notion of “mismatch” on PV systems is explained. In function of  
68 these several thermal tests, the fault detection method is presented to prevent all localized shading problems on  
69 PV modules. Section 3 speaks about the experimental validation of the detection method on PV module. Several  
70 experimentally shading tests have been performed on two PV modules, one equipped with by-pass diodes and the  
71 other not. As a result, for the both cases, I-V curves traced and analyzed for each tests of shadows on PV modules.  
72 The last section concludes this work of detection.

## 73 **2. PV systems and shadows**

74 PV systems are composed of several elements, their power production is highly dependent on weather conditions  
75 and local environment. This section introduces these elements and their relationship with the external environme  
76 nt.



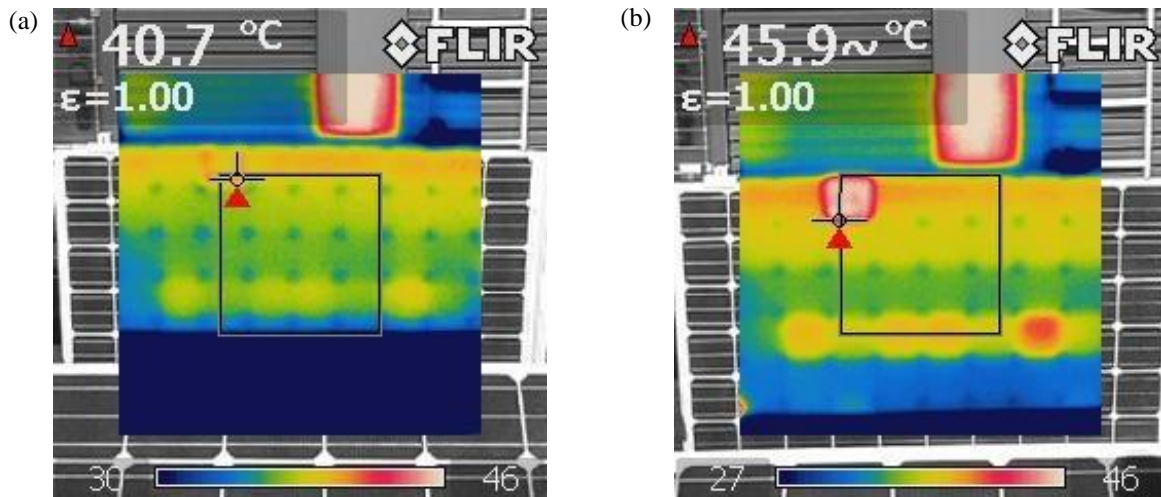


**Fig. 2 : IR camera test on PV module with a covered PV cell in open circuit (a) and in short circuit (b)**

90 Fig.1 (a) shows a homogenous temperature all over the PV module. After one hour, the initial temperature of the  
 91 PV module in open circuit is about 33°C. Temperature difference between the top and the bottom is due to the  
 92 convective effects. Maximal temperature of the PV module in this case is 37.5°. If the PV module is in short circuit  
 93 as shown in Fig. 1 (b), some PV cells starts to increase in temperature with a difference of 2°C with the first test.

94 In the next test, just one PV cell of a sub-string is completely covered. First, the PV module is in open circuit, there  
 95 is a homogenous temperature all over the PV module. The PV module is in short-circuit and after few minutes, its  
 96 temperature increase contrary to the test in Fig.1 (a) despite the PV module is in open circuit. The convective effect  
 97 has the same impact on the temperature increase visible in Fig. 2 (a). Then, the PV module is in short-circuit, a hot  
 98 spot area at level of the covered PV cell is visible in red in Fig. 2(b). After one hour, a significantly increase of  
 99 the temperature localized on the shaded PV cell is visible and it is evaluated at 45.9°. The shaded PV cell does not  
 100 receive uniform illumination contrary to the others. The current in the PV module sub-string is limited by the  
 101 shaded PV cell despite the activation of the by-pass diode of the sub-string. As a result, it operates under reverse-  
 102 bias mode, dissipating power in the form of heat.

103 To resume, non-uniform shading has an important impact on PV performances despite the activation of by-pass  
 104 diode. The IR thermography proved the presence of a hot-spot area of the shaded PV cell. It is necessary to  
 105 understand the behavior of the PV module in shading conditions. A model is developed considering the reverse  
 106 bias mode in shading conditions. This model will be used as reference in the presented fault detection method in  
 107 function of input parameters such as solar irradiation and PV cells temperature. A fault detection method is  
 108 necessary to prevent some losses related to shading problems. This work is particularly important for the diagnosis  
 109 of faults and for improving the lifetime of PV systems. Analyzing I-V curves, it gives enough information in order  
 110 to identify and to dissociate a uniform shading of a non-uniform shading. A fault detection method is developed  
 111 around of the I-V curves analysis. This work will prevent immediately when a PV module is in shading conditions  
 112 avoiding all form of dissipation. Moreover, it will allow to optimize efficiency of the PV module.

113           2.2    Solar cell model

114 The photovoltaic effect is the conversion of light into electricity. The classic model of a PV cell is governed by E  
 115 quation (1) [17-18]. Equation (1) can be used to acquire I-V curve, which shows the behavior of the current and t  
 116 he voltage of a PV system.

$$I = I_{ph} - I_0 \left[ \exp \left( \frac{q(V + I.R_s)}{nkT} \right) - 1 \right] - \frac{V + I.R_s}{R_{sh}} \quad (1)$$

117 where  $I_{ph}$  is the photocurrent (A),  $I_0$  is the dark saturation current (A),  $n$  is the ideality factor of the diode (1 to 2),  
 118  $k$  is the Boltzmann constant ( $1.38 \cdot 10^{-23}$  J/°K),  $q$  is the magnitude of the electron charge ( $1.602 \cdot 10^{-19}$  C),  $T$  is the te  
 119 mperature of the cell (°C),  $R_s$  is the series resistance,  $R_{sh}$  the shunt resistance.

120 However, most of the models in the literature do not take into account the effect of the reverse bias. A more precise  
 121 model is proposed by Bishop [19] which incorporates the avalanche effect as a non-linear multiplication factor  
 122 that affects the shunt resistance current term, shown below:

$$I = I_{ph} - I_0 \left[ \exp \left( \frac{q(V + I.R_s)}{nkT} \right) - 1 \right] - \frac{V + I.R_s}{R_{sh}} - \underbrace{a \frac{V + I.R_s}{R_{sh}} \left( 1 - \frac{V + R_s.I}{V_{br}} \right)^{-m}}_{\text{Multiplication factor on shunt resistance}} \quad (2)$$

123  
 124 where  $a$  and  $m$  are constant,  $V_{br}$  is the avalanche breakdown voltage (V).

125 By studying different PV cells in reverse bias, Bishop has noted a different evolution of the current. The avalanche  
 126 breakdown in reverse bias is shown in red in Equation (2). Negative voltages for solar cells can occur at non-  
 127 uniform illuminated PV generators, especially during partial shading of PV modules. The breakdown voltages for  
 128 poly-Si cells are within the range -12 V to -20 V, whereas for mono-Si cells the breakdown voltages can extend -  
 129 12V to -30V [20]. More precisely, when the PV module is partially shaded, the behavior of the I-V curve is  
 130 different showing the reverse bias contrary to classic equation.

131 Fig. 3 shows I-V curves model for a generic PV cell with different illumination showing the avalanche effect of  
 132 the PV cell in reverse bias. The breakdown voltage of the PV cell is estimated at -15V.

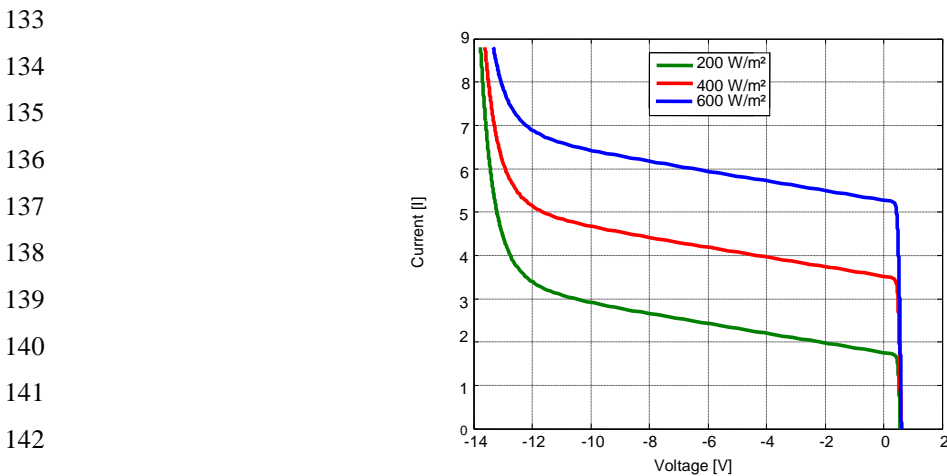


**Fig. 3 : The I-V curves for different illuminations**

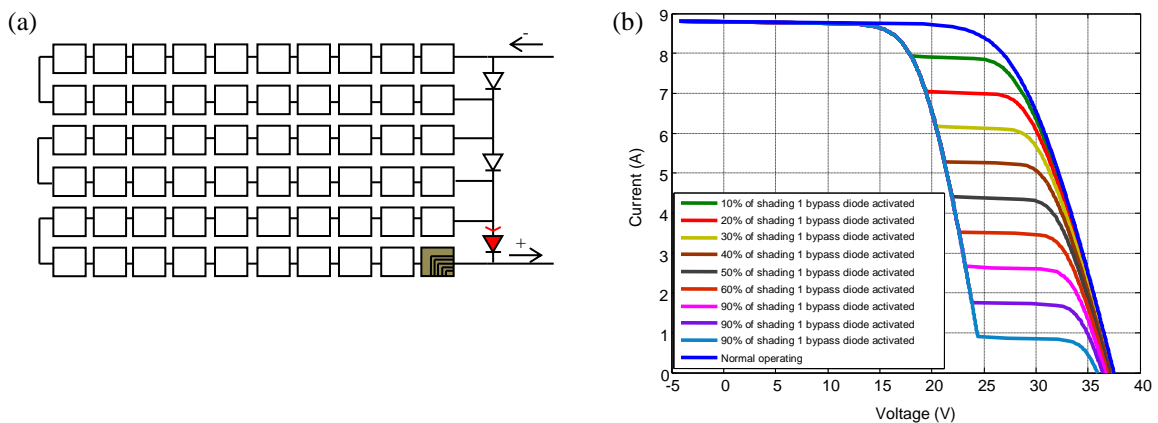
144 Several studies have analyzed these curves in detail such as [17] and [18]. In this work, a PV cell or plant is consi  
 145 dered as partially shaded when a certain percentage of its surface is covered by a shadow. As a result, shaded cell  
 146 s are forced to work in series with illuminated cells. Either each cell receives the same illuminated cells and oper  
 147 ates at a lower current leading to a lower power production, or the short circuit current of the shaded cells is less t  
 148 han the string current so that it is operated at the reverse characteristic, causing power to be dissipated and event  
 149 ually the creation of hot-spots [21]. This phenomena causes permanent losses and reduces the reliability of the sy  
 150 stem as shown with the thermography tests (Fig. 1 and in Fig.2).

### 151 2.3 Partial shading and bypass diodes

152 The solution used by the industry to protect the PV systems from partial shading is to equip them with bypass  
 153 diodes. These diodes become biased when the voltage of the shaded PV cells becomes negative. This creates a  
 154 short-circuit which limits the reverse voltage in the shaded cells [22].

155 Each cell group is protected by its own bypass diode, which has a protection threshold. This threshold limits the  
 156 bias voltage of the shaded cells and therefore the dissipated power. When diodes detect a negative voltage, shaded  
 157 cells are protected thanks to diodes activation. The threshold is estimated approximately at -0.6V.

158 The model of I-V curve of this PV module is shown in Fig. 4 (a) for different percentage of shadows performed  
 159 on one cell. If the string voltage exceeds the transmission voltage of the by-pass diode, it becomes active and short-  
 160 circuits the group of shaded PV cells. Theoretically, the breakdown voltage is not reached. In this simulation, there  
 161 are one sub-string by-passed by the diode and two in normal operating. This leads to the apparition of two break  
 162 points of the voltage as shown in Fig. 4 (b).



163 **Fig. 4 : Shading tests simulation (a) and I-V curves results (b)**

164 Most of the authors in the current literature works with shadows larger than a few cells [23-25]. Large shadows  
 165 may represent the passage of clouds or the movement of trees, which may be a problem for medium to large PV  
 166 plants. However, in smaller building integrated PV systems the PV plant may share the space with other objects  
 167 leading to projected shadows which may cover only corners of the PV modules, i.e. shading only a few cells.  
 168 Recurrent operation with small shadows is a subject generally overlooked by the current literature. In the previous  
 169 part, localized and non-uniform shadows proved the presence of a hot-spot area with an increased temperature of  
 170 the shaded PV cells. Despite the activation of the by-pass diode, it is shown with this temperature increase that the  
 171 shaded PV cells dissipate power in the form of heat degrading PV performances and its lifetime. In the next part,

172 a fault detection method is presented around I-V curves analysis. For this study, it is necessary to have an accurate  
 173 solar model as reference. The used I-V model performances has been evaluated and has been considered  
 174 satisfactory for the study [15].

#### 175 2.4 Method of detection of shading

176 There is a vast collection of PV fault detection methods in the current literature. Those, which focus on the  
 177 detection of shadows, can be roughly divided into power based or I-V based method. Power based detection  
 178 methods focus their attention on the impact of partial shading in PV power production. The objective of these  
 179 methods is to model the impact of the presence of the shadow over the PV plant depending on its geometric shape.  
 180 This type of detection is mostly based on the precise and fast modeling of the characteristics of the PV modules  
 181 [26]. This study proposes a simple mathematical model for the estimation of PV array power based on the  
 182 consideration of shading geometry. The orientation of PV modules and location of the objects which will project  
 183 shadows over the PV plant such as trees are important parameters taking into account for evaluating energy loss  
 184 [27-28]. Most authors propose models which compare I-V curves from simulations with experimental data [29-  
 185 31]. However, these methods do not give enough information about PV modules behavior and performances in  
 186 shading operating. The problematic of thermal power dissipation in shading condition is an important point to  
 187 disseminate

188

189 The proposed method in this paper revisits the idea of using a first derivative calculation to detect the presence of  
 190 a non-uniform shadows over a PV plant. Its main idea is that by monitoring the evolution of an I-V curve, it is  
 191 possible to detect the activation of bypass diodes and to clearly identify and to dissociate a non-uniform shadow  
 192 of a uniform shadow. Both don't have the same impact on PV performances and on its lifetime and this work  
 193 prevent all thermal power dissipation of the shaded PV cell. The I-V curve acquired during shading conditions is  
 194 compared to a reference I-V curve issue to a validated solar model. Their comparison is made through the  
 195 estimation of the standard error using the current from the shaded and reference I-V curves, as defined in Equation  
 196 (4).

$$E(i)_{standard} = \frac{I(i)_{reference} - I(i)_{shaded}}{\max(I(i)_{reference} - I(i)_{shaded})} \quad (4)$$

197 Where  $E(i)_{standard}$  is the standard error of the  $i$ th I-V curve point,  $I(i)_{reference}$  is the current of I-V curve under  
 198 reference conditions and  $I(i)_{shaded}$  is the current of the I-V curve acquired under shaded conditions. The standard  
 199 error is calculated for all of the points composing the I-V curve and its variation in relation to the PV voltage is  
 200 used to monitor any changes in the shaded I-V curve as a whole. This derivative is calculated through the Equation  
 201 (5).

$$\frac{dE(i)_{standard}}{dV_{module}} = \frac{E(i+1)_{standard} - E(i)_{standard}}{V(i+1)_{module} - V(i)_{module}} \quad (5)$$

202 Where  $V(i)_{module}$  is the voltage of the  $i$ th I-V curve point.



203 To validate this method, the next section will apply it to a series of I-V curves with different shading scenarios.  
 204 For each shading scenario, the evolution of the standard error will be analyzed in order to extract a general set of  
 205 interpretation rules which can be used to clearly identify some shading problems increasing the shaded PV cells  
 206 temperature. The experimental study shows the area of detection in order to dissociate the uniform-shadows of the  
 207 non-uniform shadows despite the activation of the by-pass diode.

### 208 **3. Experimental study of the detection method**

209 The experimental shading scenarios used in this section have the objective of providing a set of realistic conditions  
 210 to study the effectiveness of the new proposed detection method. These several I-V curves analysis confirm that  
 211 the shaded PV cells which is non-uniform, dissipates power in the form of heat as explained in Section 2. The  
 212 experimental setup will be presented first, giving the several shading scenarios chosen for the study. These are  
 213 followed by the analysis of the results for each shadow scenario.

#### 214 3.1 The experimental setup

215 The PV module used during these experimental tests is still the TE2200. The I-V curves are traced using the MP-  
 216 160 I-V tracer, which provides 265 measurement points between open-circuit voltage to short-circuit current. A  
 217 total of 6 sets of experimental tests were conducted to study this new detection method. Each set is composed of a  
 218 certain shading area, a shadow size and the state of the bypass diodes.

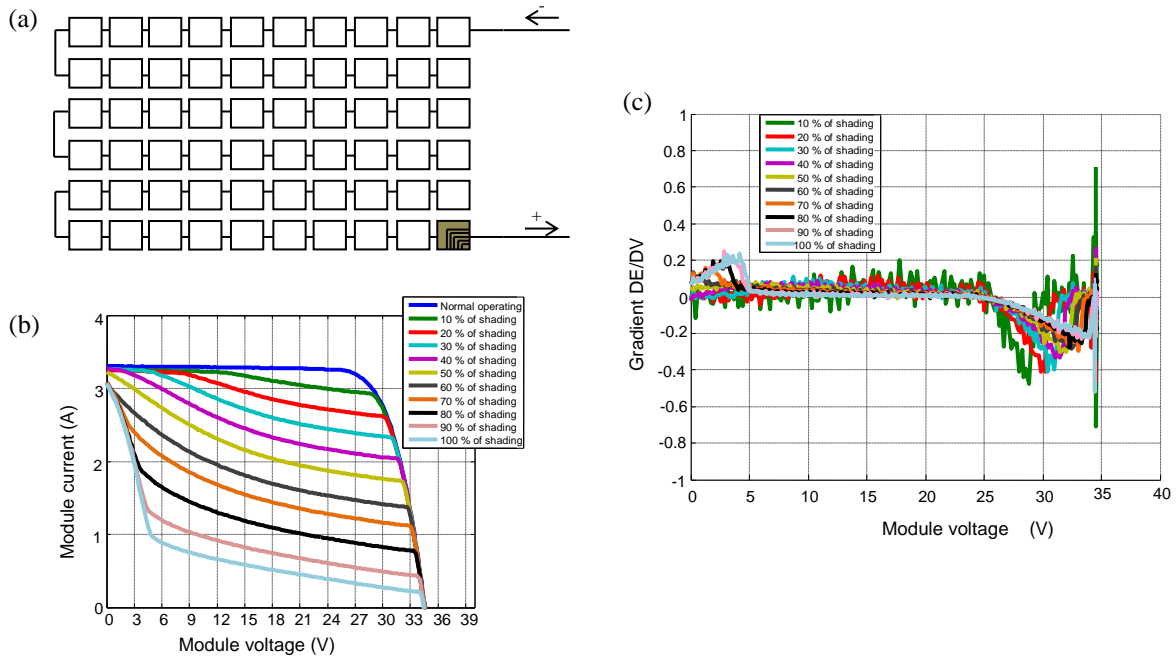
219 The shading set 1 was chosen to clearly study how the detection method reacts to the presence of the non-uniform  
 220 shadow on PV module without by-pass diodes. The shading set 2 is studied in comparison with the shading set 1  
 221 to study the difference between the activation of the bypass diodes and the presence of a localized shaded PV cell  
 222 without by-pass diode. The shading set 3 studies how the detection method can identify a homogeneous shadow  
 223 with the activation of one by-pass diode. Thus, the shading size used is 20 cells all of which have 50% of their  
 224 area shaded. The shading set 4 and 5 study the activation of 2 bypass diodes. The shadow used in these cases  
 225 covers two cells on the interface between two PV cell groups protected each by a different bypass diode. The  
 226 shading area of the set 4 is chosen to be 50% to simulate a shading scenario while the shading area of 100% in set  
 227 5 represents another case of non homogenous shading. Finally, the shading set 6 studies the detection of a  
 228 homogeneous shadow which activates two bypass diodes. It shares the same characteristics of the shading set 3.  
 229 An overview of the shading scenarios used in this study is given in Table 2.

230 **Table 2 : Scenarios of shading sets performed over PV module equipped or not of bypass diodes**

Shading Set	Shading Area	Shadow Size	Bypass Diodes
1	Variable (10% - 100%)	1 Cell	Removed
2	Variable (10% - 100%)	1 Cell	1 Active
3	Fixed (50%)	20 Cells	1 Active
4	Fixed (50%)	2 Cells	2 Active
5	Fixed (100%)	2 Cells	2 Active
6	Fixed (50%)	40 Cells	2 Active

231 3.2 Shading set 1 – Overall study of the presence of the reverse bias on I-V curves of the  
 232 PV shaded cell

233 The results for the shading set 1 are given in Fig 5. The shadow scenario is shown in Fig. 5 (a), which represents  
 234 the variation of the shading area. The presence of the reverse bias characterized by the avalanche effect and caused  
 235 by each shadow is visible on I-V curves in Fig. 5 (b). The results of the detection method are shown in Fig. 5 (c).



236 **Fig. 5 : Results for the shading set 1: (a) the shadow scenario, (b) the I-V curves for each shadow scenario and (c) the**  
 237 **results of the detection method.**

238 In Fig. 5 (b), the avalanche breakdown of the shaded PV cell is more visible on I-V curves with an high percentage  
 239 of shading on PV cell. The I-V curve slope for 100% of shading strongly changes contrary to 10% of shading. As  
 240 a result, this slope characterizes this avalanche effect of the shaded PV cells which dissipate power in the form of  
 241 heat damaging PV module on the long term and reducing its lifetime. The results from the detection method in  
 242 Fig. 5 (c) shows two areas of interest, the first from 0V to 5V and the second from 25V to 35V. The first area (0-  
 243 5V) has a positive peak that rises with the shading area. This peak is clearly caused by the presence of the avalanche  
 244 effect and represents a growing error in comparison with the reference. A growing error at such low voltages could  
 245 be interpreted as a shadow that has an overall impact on the power production, in this case due to the absence of  
 246 the bypass diodes. The second area of interest in Fig. 5 (c) (25V-35V) shows a negative peak that becomes lower  
 247 with the shading area. This peak shows that the error is becoming lower as the voltage is close to the open-circuit  
 248 voltage. In normal operating conditions, the bypass diodes will be connected and operational.

### 249 3.3 Shading set 2 – Bypass diodes and non homogenous shadows

250 In the shading set 2, the bypass diodes are connected. The shadow and active bypass diode are shown in Fig. 6 (a).  
 251 The effect of the shadow over the I-V curve is shown in Fig. 6 (b) while the results of the detection method are  
 252 shown in Fig. 6 (c).

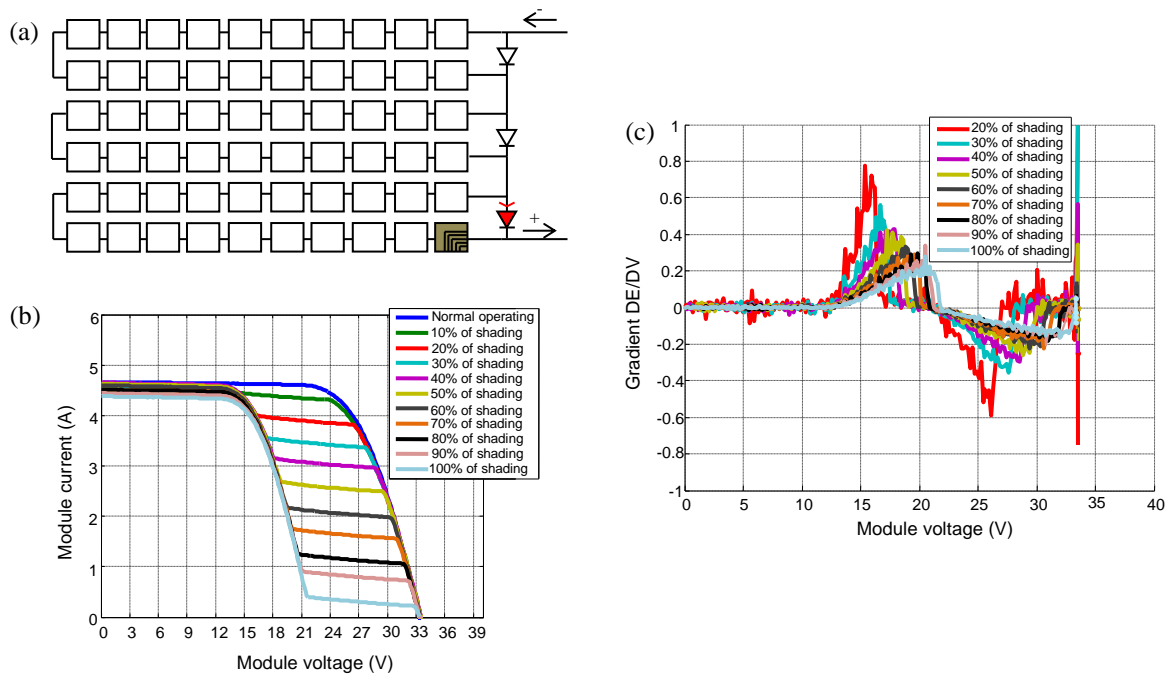


**Fig. 6 : Shading set 2 operation over PV modules (a), I-V curves results (b) and first derivative results (c)**

253

254

255

256

257

258

259

260

261

262

263

264

265

266

267

268

269

270

271

By comparing Fig. 5 (b) and Fig. 6 (b), it is possible to see that the presence of the bypass diode introduces a step. The slight slope present in Fig. 6 (b) between 15V to 33V for the different shading scenario shows that the shaded cell is a non homogenous shading. Moreover, this slope characterizes a part of the avalanche breakdown of the PV shaded cell despite the activation of the by-pass diode. In the point of view of I-V curves, this means the shaded PV cell dissipates power in the form of heat despite the activation of the by-pass diode. It is the detection of this kind of operating condition, the main objective of the new proposed method. The results shown in Fig. 6 (c) also have two areas of interest, the first from 14V to 21V and the second from 21V to 33V. The first area of interest (14V-21V) shows a positive peak whose value decreases with the shading area. An abrupt positive change in the variation of the error is linked to the presence of the shadow, as described in the shading set 1. However, in this shading set the positive peak is located at a higher voltage giving a clear indication of the correct operation of the bypass diode. By comparing the first area of interest in Fig. 5 (c) and Fig. 6 (c), it is clear that the correct operation of the bypass diode can be directly linked to the voltage in which the positive peak appears. The second area of interest (21V-33V) shows a negative peak whose value decreases with the shading area. This behavior is similar to the one observed for the second area of interest in Fig. 5 (c) and validates the impact of a non homogenous shadows despite the activation of the bypass diode. The cross comparison of the results from the shading sets 1 and 2 shows that positive peaks are linked to the bypass diodes activation with the presence of the avalanche effect characterizing a non homogenous shading. To validate this idea, the shading set 3 will study the presence of these peaks with this time an uniform shading test.

272

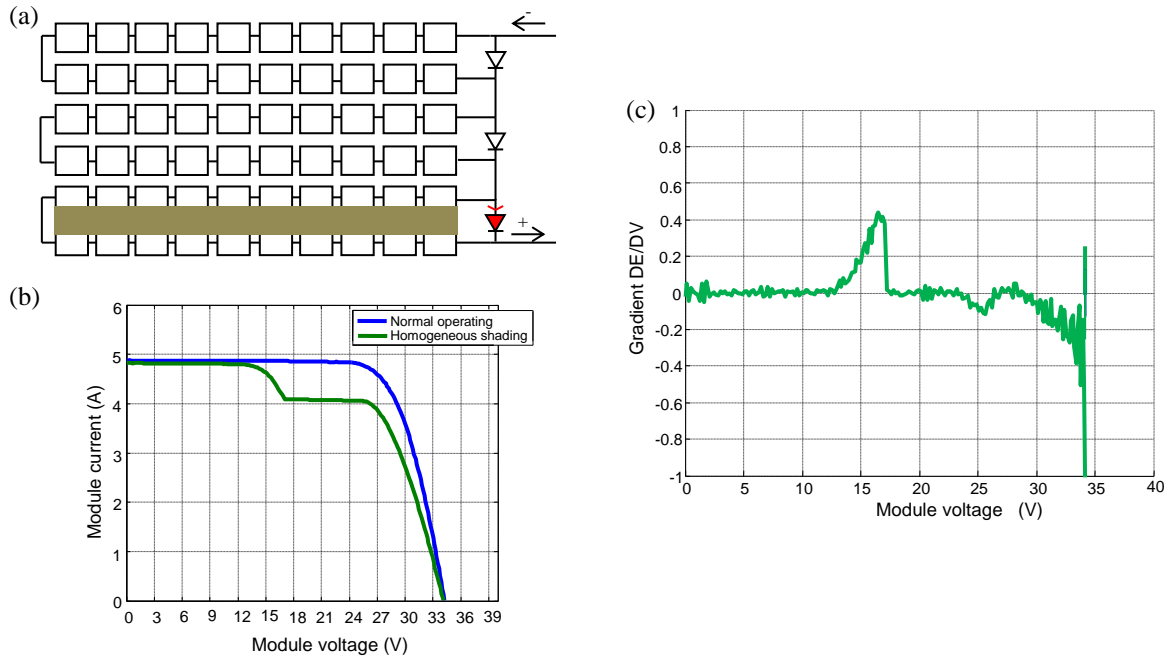
### 3.4 Shading set 3 – Bypass diodes and homogenous shadows

273

274

275

The shading set 3 shows how the detection method reacts to the activation of the bypass diode with an homogenous shadow. The shadow shape and active bypass diode are shown in Fig. 7 (a). The effect of the shadow over the I-V curve is shown in Fig. 7 (b) while the result of the detection method is shown in Fig. 7 (c).



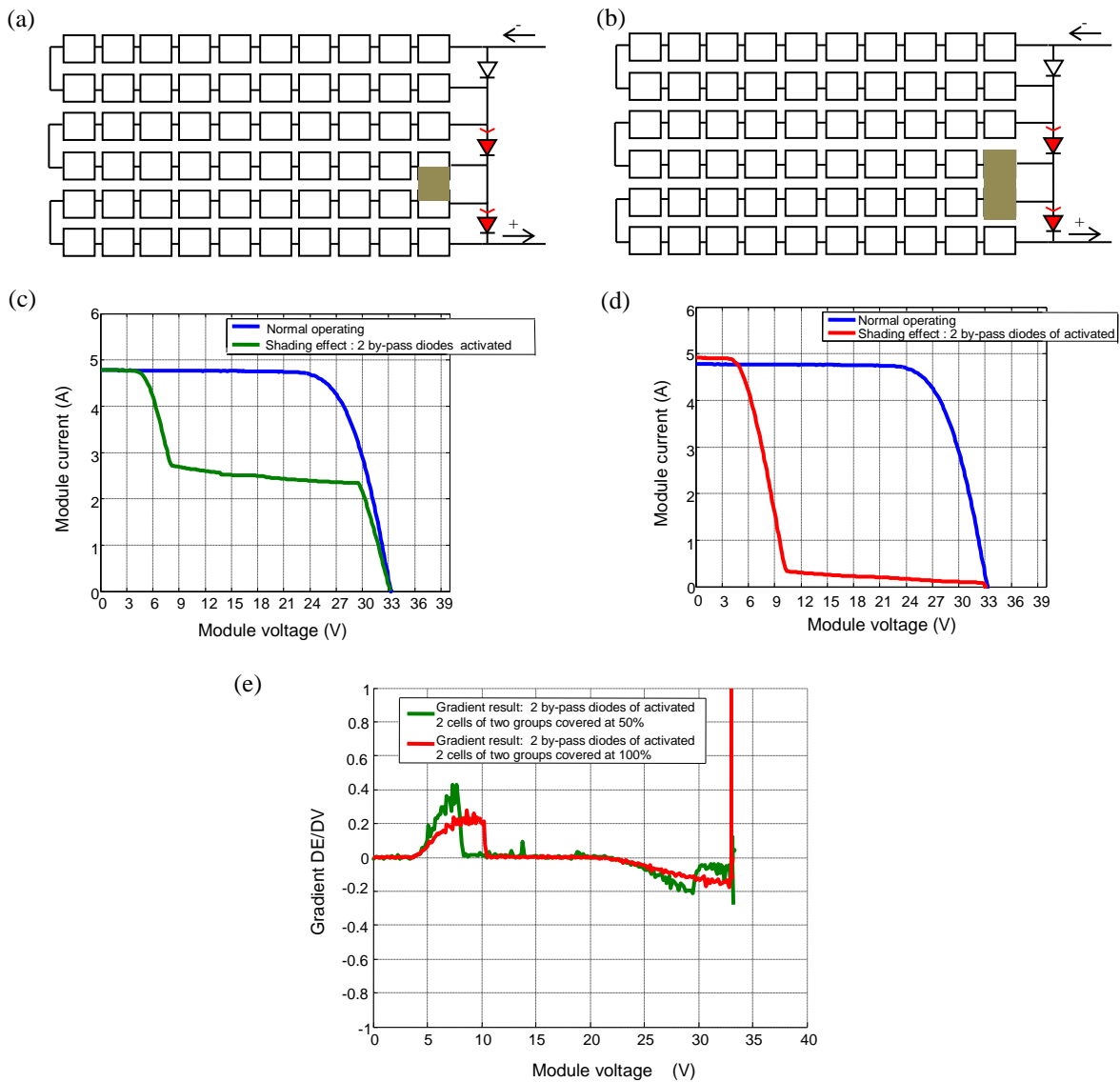
276 **Fig. 7 : Shading set 3 – (a) the shadow shape, (b) the impact of the shadow over the I-V curve and (c) the result from**  
 277 **the detection method**

278 Clearly, the slope of the region situated between 15V and 27V is less pronounced than the slope visible in Fig 6  
 279 (b). This means that it is possible to distinguish an uniform shadows of a non uniform shadow. Moreover, the  
 280 presence of this pronounced slope shown in Fig. 6 (b) is due to the avalanche effect of the shaded PV cell. By  
 281 supposition, this shaded PV cell could dissipate a part of the DC power of others cells despite the activation of the  
 282 by-pass diode. As a result, it is essential to avoid this phenomena and to prevent against non homogenous shading.  
 283 The result in Fig. 7 (c) shows a clear positive peak from 12V to 17V and two noisy negative peaks around 25V  
 284 and 33V. In this case, the shadow can be considered as homogeneous over the whole PV cell group, which means  
 285 that the avalanche effect can be almost neglected. In the absence of this avalanche effect, the positive peak prevails  
 286 over the two small negative peaks showing that the protection provided by the bypass diode can be considered as  
 287 enough. This result validates the link between the positive peaks and the bypass diodes as well as the link between  
 288 the negative peaks and the avalanche effect of the shaded PV cells. Now, three others cases where the number of  
 289 bypass diodes is different will be used to study how this new method can be used to detect the number of active  
 290 bypass diodes and their effectiveness.

### 291 3.5 Shading sets 4 and 5 – Several bypass diodes and non homogenous shadows

292 The shading set 4 and 5 seek to study how the activation of several bypass diodes can be detected by the proposed  
 293 method and if the non homogenous shading effect can still be distinguished under these shading conditions. Thus,  
 294 the shadow shape in these cases is located in the interface between two PV cell groups, forcing the activation of  
 295 two bypass diodes. The shadow shape and active bypass diode are shown in Figs. 8 (a) and 8 (b). The effect of the  
 296 shadow over the I-V curve is shown in Figs. 8 (c) and 8 (d) and the results of the detection method are shown in  
 297 Fig. 8 (e).

298



300 **Fig. 8 : Shading sets 4 and 5 – (a) and (b) the shadow shape, (c) and (d) the impact of the shadow over the I-V curves,**  
 301 **(e) the results from the detection method.**

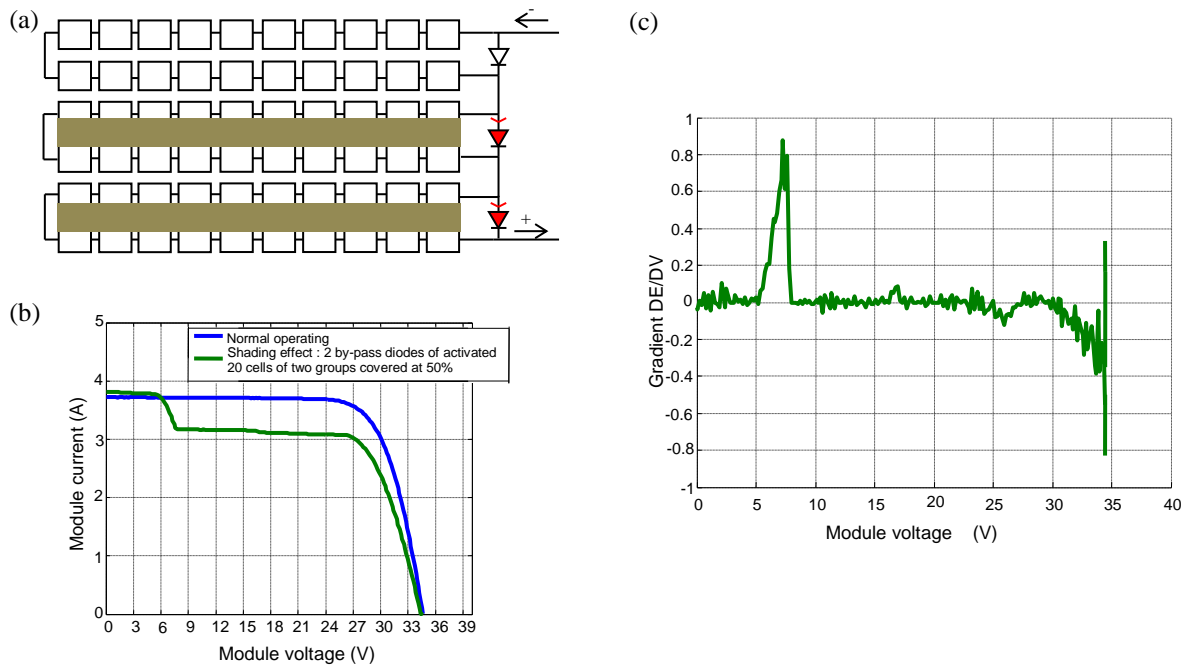
302 The results shown in Fig. 8 (e) validate the two areas of interest observed in Figs. 5, 6 and 7.

303 The first area of interest is located from 5V to 10V and has two positive peaks whose value decreases with the  
 304 shading area. These results confirm the link between positive peaks and the activation of bypass diodes. The  
 305 occurrence of these peaks at a lower voltage also indicates that a higher number of bypass diodes is active and, by  
 306 consequence, that the shadow is covering a larger part of the PV module.

307 The second area of interest is located from 21V to 33V with the two negative peaks representing the presence of  
 308 the non uniform shading visible by the slope more pronounced (9V to 30V) in Fig 8 (d) and (e). This result also  
 309 confirms the link between negative peaks and the avalanche effect of the shaded PV cells due to a non homogenous  
 310 shading. The appearance of these negative peaks at similar voltages than those in Figs. 6 and 7 indicates that the  
 311 same principle can be used to detect the presence of a shading no matter the size of the shadow such as soiling.

312 3.6 Shading set 6 – Large homogeneous shading

313 The shading set 6 has the objective of confirming the detection of the activation of bypass diodes for larger shadows  
 314 without pronounced slope visible in Fig. 8 (c) between 9V and 30V. The shadow is shown in Fig. 9 (a), its effect  
 315 in the I-V curve is shown in Fig. 9 (b) and the results from the detection method are shown in Fig. 9 (c).



316 **Fig. 9 : Shading set 6 – (a) the shadow scenario, (b) the impact of the shadow over the I-V curve and (c) the results**  
 317 **from the proposed detection method.**

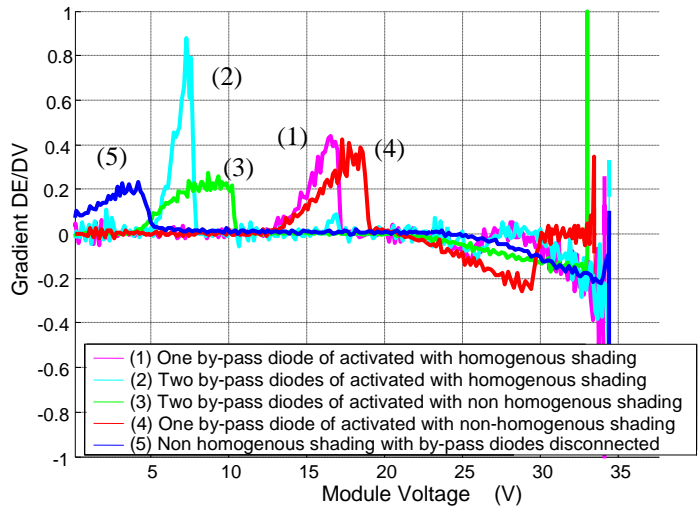
318 The result from Fig. 9 (c) confirms that a positive peak is directly linked to the activation of bypass diodes. When  
 319 a positive peak appears at voltages much lower than the open-circuit voltage, it means that the shadow is large and  
 320 several bypass diodes are active. Since the negative peak is very close to the open-circuit voltage, it can be  
 321 interpreted that the shadow is homogeneous without a pronounced slope in the region between 8V and 27V.

### 322 3.7 Summary of the experimental study

323 To summarize the results from the experimental study, Fig. 10 shows the results from the detection method for  
 324 several shading cases.

325

326  
327  
328  
329  
330  
331  
332  
333  
334



335 **Fig. 10 : First derivative calculation of the standard error compared to**  
336 **PV module voltage for each tests of shading on PV module**

336 The results validate the idea that positive peaks are associated with the activation of bypass diodes and negative  
337 peaks are associated with the presence of the avalanche breakdown of the shaded PV cells on I-V curves due to a  
338 non homogenous shading.

339 The positive peak shifts to lower voltage values as the shadow area becomes wider and more bypass diodes become  
340 active, as can be seen in cases 1 through 4 in Fig. 10. In case 5, where no bypass diode is activated, there is a  
341 positive peak close to the short circuit current, further corroborating the avalanche breakdown in reverse bias of  
342 the shaded PV shaded cells. The negative peak shifts to voltage values close to the open-circuit voltage for severe  
343 cases of non-uniform shading. Since all the negative peaks have a similar point of origin (around 20 V) it is the  
344 distance between these two points that can be used to determine the severity of the presence of this avalanche  
345 effect and more particularly the presence of a non-homogenous shading. For each shading set, different areas are  
346 visible and may be dissociated in order to perform the fault detection. This fault detection method could be  
347 implemented in a microcontroller and in embedded system. The position of the maximum amplitude in each case  
348 of shading set is different whether in the positive side than the negative side in function of the PV module voltage

349 An important remark is that the noise can be an issue when evaluating the presence of the peaks and their  
350 occurrence. To avoid false detections, it is recommended to establish an uncertainty zone around zero dE/dV and  
351 around  $V_{OC}$ . Peaks within these areas do not bring useful information to the detection and should be ignored. To  
352 summarize this part, for each shading set, an area on the calculation of DE/DV have been identified in order to  
353 detect and to dissociate a non-uniform shading of an uniform shading despite the activation of the bypass diode.  
354 The presence of the avalanche breakdown on I-V curves when the by-pass diode is activated and the non  
355 homogenous shading could have an impact on aging PV modules. Indeed, this pronounced slope traduces the fact  
356 that the shaded PV cells could dissipate power and could have important impact on the PV modules lifetime and  
357 on their effectiveness.

#### 358 **4. Conclusion**

359 The shading effect on PV module is one of the main causes of inefficiency and degradation of PV modules losses.  
360 It is difficult to quantify precisely the resulting losses and the impact on PV module aging, especially in urban

361 areas. Despite the use of by-pass diodes to protect PV modules, the presence of the avalanche effect of the shaded  
362 PV cell is visible on experimental I-V curves test with non-homogeneous shading. Some localized shaded PV cell  
363 dissipate power in the form of heat as shown in Section 2. It is shown in this study the possibility to detect and to  
364 disseminate shading forms which have not the same impact on the long term on PV modules performances for  
365 example for the case of the presence of soiling. As a result, this phenomenon could impact the PV module  
366 performance and could probably accelerate its premature aging.

367 This study has shown that it is possible to detect and identify the avalanche effect of the shaded PV cell through  
368 the presented analysis of I-V curves. Moreover, it is possible to dissociate a homogenous shading of a non  
369 homogenous shading. Several shading sets were performed on a PV module to validate the detection method  
370 proposed in this work. This method is based on the comparison of I-V curves obtained in normal operating  
371 conditions with those obtained under shading conditions. The first derivative calculation between the standard  
372 error and the PV module voltage can detect the activation of bypass diodes or other effects such as the dissipation  
373 power due to non homogenous shading on PV modules.

## 374 **5. Acknowledgements**

375 It exists a real interest to deepen this work. It will be interested to implement this method of fault detection in an  
376 embedded system. To avoid the use of solar model and additional sensors, the I-V curve reference may be the  
377 lasted data stored in memory to compare with the one in real time. The first perspective is to investigate the  
378 development of an I-V curve tracer in real time and in low power without perturb the PV production. This would  
379 permit to validate this analysis in real condition. The complexity to develop it for a PV chain is a technological  
380 research subject at investigate. The second perspective is to verify the relevance of this fault detection method  
381 through PV modules connected in series analysis.

382

## 383 **References**

- 384 [1] M.C Alonso-Garcia, J.M Ruiz, F. Chen lo, "Experimental study of mismatch and shading effects in the I-V  
385 characteristic of a photovoltaic module", *Solar Energy Materials & Solar Cells* 90, 2006, 329-340
- 386 [2] A. Woyte, J. Nijs, R. Belmans, "Partial shadowing of photovoltaic arrays with different system configurations:  
387 literature review and field test results", *Solar Energy*, Volume 74, Issue 3, March 2003, Pages 217-233
- 388 [3] Y. Sun, X. Li, R. Hong, H. Shen, "Analysis on the Effect of Shading on the Characteristics of Large-scale on-  
389 grid PV System in China", *Energy and Power Engineering*, 2013, 5, 215-218
- 390 [4] E. Lorenzo, R. Moreton, I. Luque, "Dust effects on PV array performance: in-field observations with non-  
391 uniform patterns", *PROGRESS IN PHOTOVOLTAICS: RESEARCH AND APPLICATIONS*, Prog. Photovolt:  
392 Res. Appl. 2014; 22:666–670, online library.
- 393 [5] C. Deline, B. Marion, "A performance and Economic analysis of distributed Power Electronics In Photovoltaic  
394 systems", NREL, prepared under Task No. PVD9.1410.
- 395 [6] F. Mejia, J. Kleissl, J.L. Bosch, The Effect of Dust on Solar Photovoltaic Systems, *Energy Procedia*, Volume  
396 49, 2014, 2370-2376
- 397 [7] A. Sayyah, M. N. Horenstein, M. K. Mazumder, "Energy yield loss caused by dust deposition on photovoltaic  
398 panels", *Solar Energy*, Volume 107, September 2014, Pages 576-604



399 [8] Julius Tanesab, David Parlevliet, Jonathan Whale, Tania Urmee, Trevor Pryor, "The contribution of dust to  
400 performance degradation of PV modules in a temperate climate zone", *Solar Energy*, Volume 120, October 2015,  
401 147-157

402 [9] Soteris A. Kalogirou, Rafaela Agathokleous, Gregoris Panayiotou, On-site PV characterization and the effect  
403 of soiling on their performance, *Energy*, Volume 51, 1 March 2013, 439-446

404 [10] S. Silvestre, A. Boronat, A. Chouder, "Study of bypass diodes configuration on PV modules", *Applied*  
405 *Energy*, Volume 86, Issue 9, September 2009, 1632–1640

406 [11] Y. Zhao, B. Lehman, R. Ball, J. Mosesian, J. F. de Palma, "Outlier detection rules for fault detection in solar  
407 photovoltaic arrays", *Applied Power Electronics Conference and Exposition (APEC), 2013 Twenty-Eighth Annual*  
408 *IEEE*, 2913 - 2920

409 [12] T. Takashima, J. Yamaguchi, K. Otani, K. Kato, and M. Ishida, "Experimental studies of failure detection  
410 methods in PV module strings", *Photovoltaic Energy Conversion, Conference Record of the 2006 IEEE 4th World*  
411 *Conference*, Page(s): 2227-2230

412 [13] Y. Hirata, S. Noro, T. Aoki, and S. Miyazawa, "Diagnosis Photovoltaic Failure by Simple Function Method  
413 to Acquire I-V Curve of Photovoltaic Modules String", *Photovoltaic Specialists Conference (PVSC), 2012 38th*  
414 *IEEE*, Page(s): 1340-1343

415 [14] M. Bressan, Y. El-Basri, C. Alonso, "A new method for fault detection and identification of shadows based  
416 on electrical signature of defects," in *Power Electronics and Applications (EPE'15 ECCE-Europe), 2015 17th*  
417 *European Conference on* , vol., no., pp.1-8, 8-10 Sept. 2015

418 [15] Y. El Basri, M. Bressan, L. Seguier, H. Alawadhi, C. Alonso, "A proposed graphical electrical signatures  
419 supervision method to study PV module failures", *Solar Energy*, Volume 116, June 2015, Pages 247-256

420 [16] Riley, Cameron William, "An Autonomous Online I-V Tracer for PV Monitoring Applications. " Master's  
421 Thesis, University of Tennessee, 2014.

422 [17] G. Walker "Evaluating MPPT converter topologies using a MATLAB PV model", *J. Electr. Electron. Eng.*  
423 *Aust.*, vol.21, no. 1, pp 49-56, 2001

424 [18] M.G. Villalva, J. R. Gazoli, E. R. Filho, "Comprehensive approach to modeling and simulation of photovoltaic  
425 arrays", *IEEE transactions on power electronics*, Vol. 24, NO. 5, May 2009

426 [19] J.W Bishop, "Computer Simulation of the effects of electrical mismatches in photovoltaic cell interconnection  
427 circuit", ESTI Project, Commission of the European Communities Joint Research Centre, 1988.

428 [20] W. Hermann, W. Wiesner, W. Vaaben, "Hot spot investigations on PV modules-new concepts for a test  
429 standard and consequences for module design with respect to bypass diodes", *Photovoltaic Specialists Conference*,  
430 1997., *Conference Record of the Twenty-Sixth IEEE*, Page(s): 1129-1132

431 [21] Solórzano, J., Egido, M.A., 2013. "Automatic fault diagnosis in PV systems with distributed MPPT". *Energy*  
432 *Convers. Manage.* 76, 925–934.

433 [22] Tae Hee Jung, Jae Woo Ko, Gi Hwan Kang, Hyung Keun Ahn, "Output characteristics of PV module  
434 considering partially reverse biased conditions", *Solar Energy*, Volume 92, June 2013, Pages 214-220

435 [23] Patel H, Agarwal V. "Maximum power point tracking scheme for PV systems operating under partially shaded  
436 conditions". *IEEE Trans Industr Electron* 2008;55(4):1689–98

437 [24] Bidram A, Davoudi A, Balog RS. "Control and circuit techniques to mitigate partial shading effects in  
438 photovoltaic arrays". *IEEE J Photovoltaics* 2012;2:532–46.

- 439 [25] M. L. Orozco-Gutierrez, J. M. Ramirez-Scarpetta, G. Spagnuolo, and C. A. Ramos-Paja, "A method for  
440 simulating large PV arrays that include reverse biased cells," *Applied Energy*, vol. 123, pp. 157–167, Jun. 2014.
- 441 [26] F. Martínez-Moreno, J. Muñoz, E. Lorenzo, "Experimental model to estimate shading losses on PV arrays",  
442 *Solar Energy Materials & Solar Cells* 94 (2010) 2298–2303
- 443 [27] M. Drif, A. Mellit, J. Aguilera, P. J. Pérez, "A comprehensive method for estimating energy losses due to  
444 shading of GC-BIPV systems using monitoring data", *Solar Energy* 86 (2012) 2397–2404
- 445 [28] L. Sun, L. Lu, H. Yang, "Optimum design of shading-type building-integrated photovoltaic claddings with  
446 different surface azimuth angles", *Applied Energy* 90 (2012) 233–240
- 447 [29] M.C. Alonso-García, J.M. Ruiz, W. Herrmann, "Computer simulation of shading effects in photovoltaic  
448 arrays", *Renewable Energy*, Volume 31, Issue 12, October 2006, Pages 1986-1993
- 449 [30] Engin Karatepe, Mutlu Boztepe, Metin Çolak, "Development of a suitable model for characterizing  
450 photovoltaic arrays with shaded solar cells", *Solar Energy*, Volume 81, Issue 8, August 2007, Pages 977-992,
- 451 [31] Hajime Kawamura, Kazuhito Naka, Norihiro Yonekura, Sanshiro Yamanaka, Hideaki Kawamura, Hideyuki  
452 Ohno, Katsuhiko Naito, "Simulation of I–V characteristics of a PV module with shaded PV cells", *Solar Energy*  
453 *Materials and Solar Cells*, Volume 75, Issues 3–4, 1 February 2003, Pages 613-621